

Simulating Urban Environments for Energy Analysis

G. H. Weber^{1,2} H. Johansen¹, D. T. Graves¹ and T. J. Ligocki¹

¹Computational Research Division, Lawrence Berkeley National Laboratory, USA

²Department of Computer Science, University of California, Davis, USA

Abstract

We present new prototype tools for optimizing building solar energy impacts in urban regions, to enable better real-time control and policy decisions for energy supply and demand response. The concept is demonstrated with a prototype that estimates the amount of direct sunlight available to building surfaces in complex urban landscapes, taking into consideration local weather predictions (via cloud cover simulation). We also calculate partial shadows from visual obstructions, due to their effect on the availability of solar energy and building energy usage. The prototype has the potential to make better day-ahead predictions that can help balance energy supply and demand during peak load hours. This can lead to better strategies for control of heating, air conditioning and alternatives (such as local energy storage in batteries or co-generation) to offset peak energy demand. However, in addition it can be used as a statistical optimization tool for informing local policy decisions related to solar energy incentives and demand response programs. We apply the approach to a prototype calculation on models of a hypothetical city and a section of downtown San Francisco. We briefly discuss optimization opportunities in response to the variability and uncertainty in solar energy for individual buildings in an urban landscape.

Categories and Subject Descriptors (according to ACM CCS): I.3.8 [Computer Graphics]: Applications—I.6.3 [Simulation and Modeling]: Applications—J.7 [Computers In Other Systems]: Computer Applications—

1. Introduction and Related Work

The complexity of urban power supply and demand is growing rapidly with the diversity of technologies that participate in energy systems. For example, the inclusion of renewables (especially solar and wind energy), demand response, electric vehicles, combined heat and power systems, battery storage, must coexist with existing generation capacity. Strategies have to be developed that do not exacerbate issues like grid outages, single points of failure, or that miss energy savings and investment opportunities. However, in many cases a leading factor that drives that energy balance for electricity is the external environment: air temperature, air quality, humidity, precipitation, and most importantly, incident sunlight, shade and cloud cover. These weather-related factors are dominated by uncertainty and day-to-day variation, which makes optimization of energy usage, production, and storage difficult. Thus, approaches focusing on static, peak views of the system (solar angle, average hours sunlight per day) miss opportunities for to optimize supply/demand and the use of solar energy in urban areas.

The goal of this work is to provide a high-resolution simulation time series of regional weather and climate scenarios,

that can be used as part of an optimal design tool for urban energy usage and planning. To that end we have created a simplified system as a prototype, in which we:

- Perform a multi-scale simulation of key factors that affect incident solar radiation (such as cloud cover) over the urban environment;
- Calculate a time-snapshot of incident solar energy, which takes into consideration cloud cover, topography, angle of the sun, shadows, etc.;
- Generate a time-series of solar energy for each building, based on its unique surroundings; and finally,
- Use these time series data to evaluate potential for optimizing solar energy generation and electricity demand.

Regional high-resolution weather simulations have become a standard approach for short-term meteorological predictions (see, for example [WRF]). Detailed flow in urban environments is a relatively new area of research, generally focused on static calculations for urban planning (such as “wind tunnel” effects) and security (dispersion of harmful airborne contaminants) [SL10]. In general, time-dependent flows that combine architectural ($O(1m)$) and regional weather ($O(10^6m)$) scales are computationally diffi-

cult. We are using the multi-resolution adaptive mesh refinement capabilities in *Chombo* [Cho] to capture both scales in a time-dependent simulation. In addition, we are modeling the building-level flow using an incompressible flow solver for embedded boundaries [MT12]. The embedded boundary representation is very flexible, and can quickly grid complex urban environments and represent distinct surface features of each building. This level of resolution can also be the basis for calculating solar exposure of the building.

We use direct volume rendering [Lev88, Sab88, Max95]—a technique commonly employed in scientific visualization—to calculate incident solar radiation. While accurate modeling of light transport [PH04] has replaced heuristic approaches for photorealistic rendering, and tools such as Radiance [War94] simulate light conditions in buildings accurately for planning, the large scale of urban regions is prohibitive for using these approaches.

2. Approach

Our prototype system represents the geometry of the urban region as cut-cells (Section 2.1) and uses the Chombo AMR code to advect clouds over the urban region (Section 2.2). The output of this step is a 3D HDF5 file with an approximate water vapor volume fraction in each computational cell. We use VisIt [CBW*12] to compute the energy transfer through the cloud layer and shadows (Section 2.3). The result is a file with intensity values—corrected for shadow effects—at locations in the volume corresponding to building locations. Finally, our prototype uses MATLAB to compute energy transfer into buildings and clusters energy transfer profiles to obtain a set of representative energy transfer curves (Section 2.4).

2.1. Embedded Boundary Generation

In the first example, a synthetic city was generated by randomly placing 500 random size boxes over a 1km^2 area, separated by streets, across a ground height defined by four Gaussian hills. Although not a realistic city geometry, this provides enough height and spatial variation in the urban landscape to test the approach. A second example used a 3D surface triangulation of a district of San Francisco, generated from building cross-sections at evenly-spaced elevations.

In both, the landscape was represented as a level set in three dimensions, and combined using constructive solid geometry operations. Then the level set description was intersected with each computational cell to calculate geometric quantities (such as surface normals and area fractions), using the methods described in [LSPC07].

2.2. Cloud Advection Using the Chombo Code

Although it is not a full weather simulation, we chose to implement the prototype using a steady flow with random

distribution of Gaussian clouds that pass over the urban region (see Figure 1). The velocity field is evolved using an incompressible flow solver, as implemented in [MT12] to get to an approximate steady state. Because the algorithm we use includes an adaptive mesh, we can simultaneously use an embedded boundary method for the buildings (cut from an ordinary Cartesian grid [Cho]) and use coarser resolutions for the atmosphere. Here the goal is to provide a dynamic cloud layer to test the building solar intensity algorithm, which could be extended to use weather predictions or ensembles of meteorological data.

2.3. Light Intensity Computation

To approximate the light intensity shining on building in large urban regions, we make a few simplifying assumptions:

- The solar angle relative to the urban landscape is specified as a function of time, given the latitude and time of year.
- The region is so small that all light rays are parallel. The light direction depends only on time.
- Contributions of diffuse light—due to reflections within the cloud layer—to energy transfer into buildings is negligible, and it is possible to approximate light transfer through clouds using an absorption only model.
- Contributions of reflected light from other buildings to energy transfer in a building is negligible. The only noticeable effect is by casting shadows.
- The cloud layer is far above the buildings. There is no light absorption at low altitudes, e.g., due to ground-level fog.

Some of these assumptions—such as the parallel light rays—are motivated by the desire to use standard tools like VisIt [CBW*12] to develop an initial prototype and will be relaxed in future work. Our prototype approximates light intensity shining on buildings as illustrated in Figure 2. Since the cloud layer is far away from the building, we place an image plane—depicted blue in the figure—perpendicular to the light direction between the cloud layer and the buildings. To compute the fraction of light energy transmitted along the ray passing through the cloud layer and arriving at the image plane, we evaluate the emission and absorption light model [Max95] along parallel rays through the volume using VisIt’s X-ray query. The advantage of this approach is that it decouples calculations in the cloud layer from the geometry of the urban region.

To evaluate the light energy shining on buildings, we first reconstruct the geometry from a 3D CAD description, as a Chombo cut-cell representation. The ground and individual buildings are then identified using VisIt’s material interface reconstruction [MC10]. To obtain the light intensity shining onto a point on a building, we cast a ray from this point parallel to the sunlight direction and intersect it with the image plane, obtaining the appropriate fraction of light from the pixel containing the intersection point.

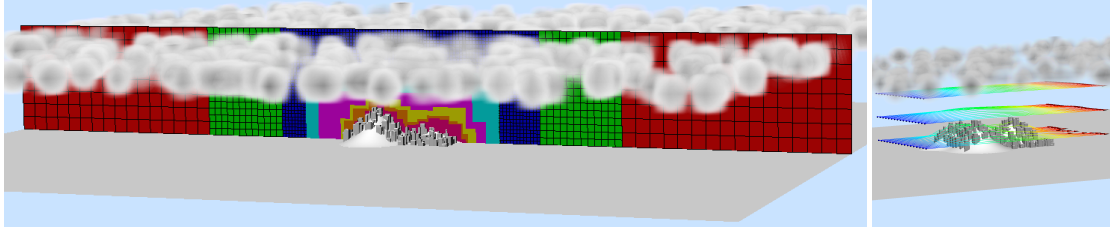


Figure 1: Advecting clouds using a Chombo-based simulation on an adaptive mesh.

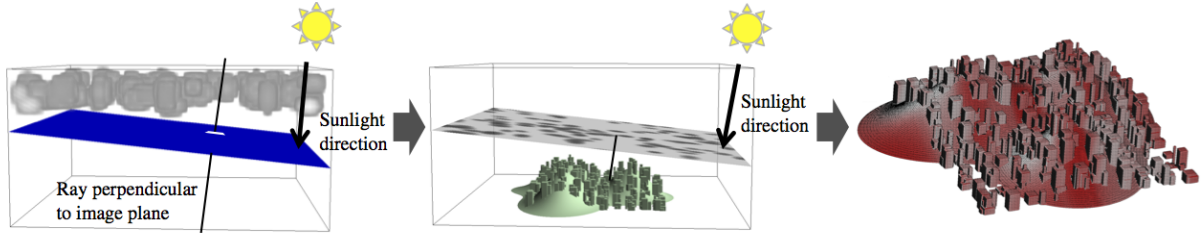


Figure 2: Computing the light intensity transferred through the cloud layer and mapping it onto the buildings.

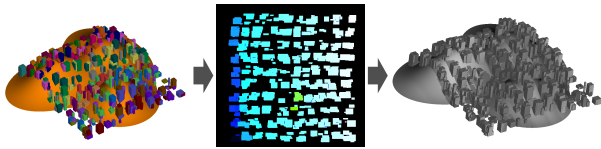


Figure 3: Computing building shadows using a hybrid of shadow and OpenGL selection buffers, with building IDs.

To determine whether another building blocks the sun, we use a hybrid approach between a shadow buffer [Wil78] and an OpenGL selection buffer [OSW*], see Figure 3. Like in the shadow buffer method, we render the scene from the point of view of the sun. Instead of distance from the light source, each pixel records the unique identification number of the building visible from the sun. We store this identifier in the three color components (red, green and blue) using eight bits per component. The result is a bitmap image where each pixel corresponding to a parallel ray contains the identifier of the building that is visible from the light source.

To combine this information with the intensity information computed using the X-ray query, we use the same way of intersecting a ray in light direction from the building with the image plane—the image planes for the shadow information and intensity information coincide. If the current building has the same ID, it receives the light intensity specified in the intensity image. Otherwise, it is in the shade and does not receive any energy directly from the sun. While this approach is prone to aliasing—due to the restricted shadow buffer resolution—we found its accuracy sufficient for approximating energy transfer into buildings.

2.4. Energy Transfer Into Buildings

Given the light intensity from 2.3, the energy transfer to any building surfaces can be calculated on a unit-area basis (I/m^2) and, if desired, for different building surfaces. The total over the entire building surface is then expressed as a time series for each building, showing incident solar energy versus time. These time series can be analyzed in various ways:

- Identifying time/duration of peak incident solar energy,
- Clustering building’s time series, or identifying outliers
- Comparing time-series to building electrical meter data,

and so on. In general, the hope is to identify which solar energy strategies are best- or poorly-suited given each of the building (or even building surface) behaviors across an ensemble of weather simulations at different times of year.

3. Results

We tested our prototype on a testbed urban model also known as “Terryville.” The simulation covers a domain of $64km^2 \times 1km$, which is within the reach of global/regional weather predictions. The finest level of the adaptive mesh refinement hierarchy is at a resolution of $1m^3$ —equivalent to 70B points without the use of AMR. Through use of AMR, we achieve a $300\times$ reduction to 200M points in an 8 level hierarchy and 2 : 1 refinement between levels. The cloud advection was computed on a 64 core cluster for this geometry, and then overlaid on a 3D model of a small district of downtown San Francisco. We then used VisIt (running on an 8 core MacBook Pro) to compute the energy transfer through clouds, and the time series of this for individual buildings.

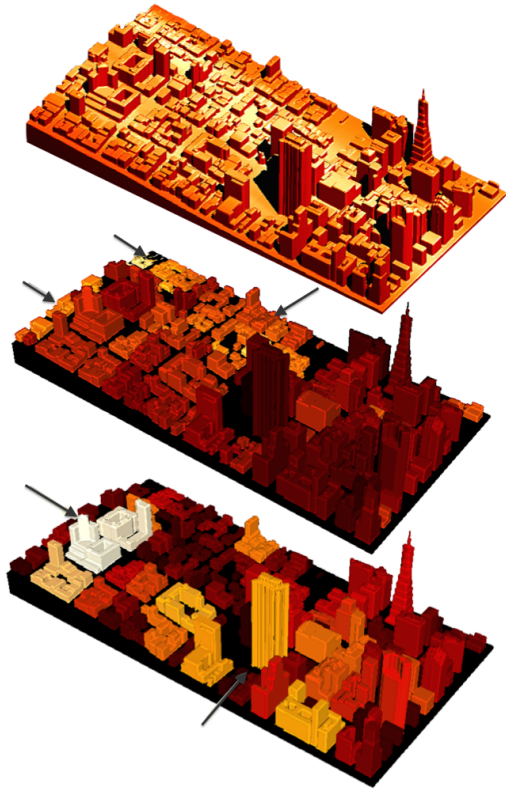


Figure 4: False color plot (top) of incident solar energy, with cloud and building shadows, for a San Francisco district at a specific time. (Middle) Lighter colors mean more energy per unit of building area, as opposed to (bottom) the total for each building. Arrows highlight districts or buildings that might be the focus of policy or demand incentives.

Figure 4 shows a point-in-time result for San Francisco, which identifies how much sunlight shines on each surface of the domain, by coloring them according to incident solar energy. The middle figure shows solar energy per unit area of a building, which could be used to identify a region with statistically less cloud cover or shadow obstructions for specific times of day. The bottom figure shows how individual buildings could be identified, where there is the greatest incident solar energy over the entire building surface area. These types of calculations could be used to prioritize solar energy incentives or establish districts where solar supply and energy demand are more balanced given local variability.

By simulating the movement of clouds throughout the day, and adjusting the sun location and shadows appropriately, we can estimate incident solar energy per unit area, shown in Figure 5. In aggregate, one can see the effect of clouds passing over the landscape (average peaks and troughs), as well as buildings that have the most and least solar exposure due to their position and height in the urban

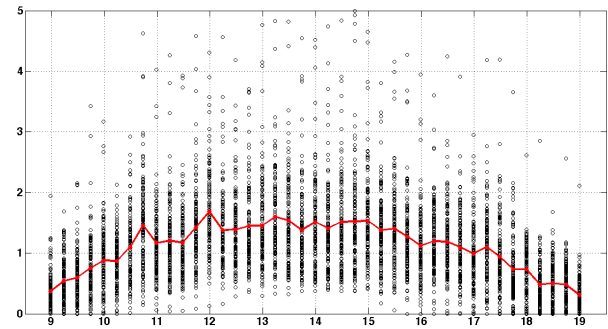


Figure 5: A scatter plot of the computed incident solar energy per unit building area (black, normalized scale) and average over all buildings (red line), versus time of day.

landscape. Figure 5 also shows outlier buildings, where their behavior is different due to their shape or orientation. Similarly, it is easy to identify clusters that are sensitive to sun orientation, where buildings obtain less incident light in the mornings or afternoons due to shadows.

4. Conclusions and Future Work

The current work served as a feasibility study—relying mostly on existing tools—and a starting point for extensive investigations of the urban environment energy system. Clearly, using models from real cities, e.g., via Google Earth or other sources, will be needed to connect to electrical grid and metering data. Similarly, integrating with a regional weather prediction code and other weather data sources would provide the basis for a policy decision tool. For example, fine-grained choices could be made, such as reducing incentives for solar panel installation in locations where fog or shade reduce generation during critical peak electrical loads. For purposes of predicting building energy consumption and urban “heat island” effects, diffuse and other indirect light—both light scattered in the clouds as well off reflective surfaces—should be considered as well, because it affects building occupancy loads for lighting and heating. In future work, we will explore using physically based rendering approaches to model the light intensity more accurately while still aiming to keep the computational complexity at level that makes large scale simulations possible.

Acknowledgements

We thank Eric Brugger for help and advice with the VisIt X-ray query. This work was supported by the Department of Energy (DOE) Office of Science, Advanced Scientific Computing Research (ASCR), under Contract No. DE-AC02-05CH11231.

DISCLAIMER

This document was prepared as an account of work sponsored by the United States Government. While this document is believed to contain correct information, neither the United States Government nor any agency thereof, nor the Regents of the University of California, nor any of their employees, makes any warranty, express or implied, or assumes any legal responsibility for the accuracy, completeness, or usefulness of any information, apparatus, product, or process disclosed, or represents that its use would not infringe privately owned rights. Reference herein to any specific commercial product, process, or service by its trade name, trademark, manufacturer, or otherwise, does not necessarily constitute or imply its endorsement, recommendation, or favoring by the United States Government or any agency thereof, or the Regents of the University of California. The views and opinions of authors expressed herein do not necessarily state or reflect those of the United States Government or any agency thereof or the Regents of the University of California.

References

- [CBW*12] CHILDS H., BRUGGER E., WHITLOCK B., MEREDITH J., AHERN S., PUGMIRE D., BIAGAS K., MILLER M., WEBER G. H., KRISHNAN H., FOGAL T., SANDERSON A., GARTH C., BETHEL E. W., CAMP D., RÜBEL O., DURANT M., FAVRE J., NAVRATIL P.: VisIt: An end-user tool for visualizing and analyzing very large data. In *High Performance Visualization—Enabling Extreme-Scale Scientific Insight*, Bethel E. W., Childs H., Hansen C., (Eds.), Chapman & Hall, CRC Computational Science. CRC Press/Francis-Taylor Group, Boca Raton, FL, USA, Nov. 2012, pp. 357–372. <http://www.crcpress.com/product/isbn/9781439875728>, LBNL-6320E. 2
- [Cho] CHOMBO: APPLIED NUMERICAL ALGORITHMS GROUP: Chombo. <https://chombo.lbl.gov/>. 2
- [Lev88] LEVOY M.: Display of surfaces from volume data. *Computer Graphics and Applications, IEEE* 8, 3 (May 1988), 29–37. 2
- [LSPC07] LIGOCKI T. J., SCHWARTZ P. O., PERCELAY J., COLELLA P.: Embedded boundary grid generation using the divergence theorem, implicit functions, and constructive solid geometry. *J. Phys.: Conf. Ser.* 125 (2007), 012080. 2
- [Max95] MAX N.: Optical models for direct volume rendering. *IEEE Transactions on Visualization and Computer Graphics* 1, 2 (Jun 1995), 99–108. doi:10.1109/2945.468400. 2
- [MC10] MEREDITH J. S., CHILDS H.: Visualization and analysis-oriented reconstruction of material interfaces. *Computer Graphics Forum (Proceedings Eurographics/IEEE Symposium on Visualization)* 29, 3 (2010). 2
- [MT12] MILLER G. H., TREBOTICH D.: An embedded boundary method for the navier-stokes equations on a time-dependent domain. *Communications in Applied Mathematics and Computational Science* 7, 1 (2012), 1–31. 2
- [OSW*] OPENGL ARCHITECTURE REVIEW BOARD, SHREINER D., WOO M., NEIDER J., DAVIS T.: *OpenGL Programming Guide*. Addison-Wesley. 3
- [PH04] PHARR M., HUMPHREYS G.: *Physically Based Rendering: From Theory to Implementation*. Morgan Kaufmann Publishers Inc., San Francisco, CA, USA, 2004. 2
- [Sab88] SABELLA P.: A rendering algorithm for visualizing 3d scalar fields. *SIGGRAPH Comput. Graph.* 22, 4 (June 1988), 51–58. URL: <http://doi.acm.org/10.1145/378456.378476>, doi:10.1145/378456.378476. 2
- [SL10] SCHATZMANN M., LEITL B.: Validation of urban flow and dispersion cfd models. In *The Fifth International Symposium on Computational Wind Engineering (CWE2010) Chapel Hill, North Carolina, USA, May 23-27, 2010* (2010). URL: ftp://ftp.atdd.noaa.gov/pub/cwe2010/Files/Papers/427_Schatzmann.pdf. 1
- [War94] WARD G. J.: The RADIANCE lighting simulation and rendering system. In *Proceedings of the 21st Annual Conference on Computer Graphics and Interactive Techniques* (New York, NY, USA, 1994), SIGGRAPH '94, ACM, pp. 459–472. URL: <http://doi.acm.org/10.1145/192161.192286>, doi:10.1145/192161.192286. 2
- [Wil78] WILLIAMS L.: Casting curved shadows on curved surfaces. *SIGGRAPH Comput. Graph.* 12, 3 (Aug. 1978), 270–274. URL: <http://doi.acm.org/10.1145/965139.807402>, doi:10.1145/965139.807402. 3
- [WRF] WRF: NATIONAL OCEANIC AND ATMOSPHERIC ADMINISTRATION (NOAA) AND NATIONAL CENTERS FOR ENVIRONMENTAL PREDICTION (NCEP): Weather Research and Forecasting. <http://www.dtcenter.org/wrf-nmm/users/>. 1